

BME Written Qualifying Exam

Colin Sullender

May 24, 2012

Question 1

A major limitation of two-photon calcium imaging is the relatively slow acquisition times that arise because of the raster-scanning illumination strategy where hundreds of thousands of spatial coordinates must be individually targeted for two-photon excitation¹⁻⁵. Calcium imaging is used to track neuronal activity by indirectly measuring changes in calcium concentration evoked by action potentials with calcium-sensitive fluorophores⁶. One of the most promising strategies for drastically improving imaging rates is the use of multifocal two-photon microscopes, where an individual laser beam is split into numerous beamlets for simultaneous illumination at multiple spatial locations within the sample⁷. In this paper, Cheng, et al. improve upon the multifocal technique by spatiotemporally multiplexing four beamlets to eliminate light-scattering ambiguity that has plagued deep-brain multifocal two-photon imaging in order to allow for greater imaging depths⁸. Previous systems have been limited to imaging depths of only $\sim 100\mu\text{m}$ because of scattering, which is insufficient for appropriately imaging neuronal activity⁹. This system is capable of imaging four different axial planes simultaneously, allowing for three-dimensional data acquisition without requiring physical movement of the objective or stage.

The individual beamlets are obtained by splitting the primary beam of an 80MHz Ti:Al₂O₃ laser into four separate beams with polarizing beam splitters and half-wave plates to control intensity (**Fig. 1**). A 3ns temporal delay is introduced between each beamlet via a $\sim 1\text{m}$ extension in path length such that the beams arrive at the objective back aperture with $t = 0\text{ns}$, 3ns , 6ns , and 9ns . The converging beams are slightly offset on the back aperture to introduce spatial separation. Two different scanning mirrors are used to raster the beamlets across the sample. A closed-loop scanning mirror is utilized for the slow scan axis while a 16kHz resonant scanning mirror is used for the fast scan axis linescans. Several different objectives were used in the system for varying imaging conditions (40x 1.0NA, 40x 0.8NA, and 60x 0.9NA). Two different calcium indicators, Fluo-4 acetoxymethyl (AM) ester and Oregon Green BAPTA-1 AM (OGB), were used during imaging. A hybrid photodetector featuring an avalanche photodiode for electron targeting rather than the usual dynode stages found in a PMT was used for detecting the resulting two-photon fluorescence^{10,11}. The temporal separation of the beamlets allowed for the use of a point detector, a significant difference from previous multifocal systems⁹. The resulting signal was then demultiplexed in time to separate the fluorescence data from each of the four beamlets, amplified, and digitized for processing. The spatial coordinates of the data is used to reconstruct the fluorescence image of the calcium indicator and individual cells located using morphological image processing. Calcium transients are identified within each cell's fluorescence trace and used to locate "peaks of synchrony" within the imaging area (cells that participate in synchronous bursts of activity)¹². The spatial distribution of cells participating in each synchronous event is then used to ascertain the movement of the neuronal event within the imaging region.

The system offers a four-fold increase in raster-scanning efficiency by simultaneously exciting four different focal volumes. This increase in temporal resolution has the added benefit of improving the overall signal-to-noise ratio and field of view¹³. The system is capable of simultaneously imaging four points on the same axial plane, two points on two different axial planes, or one point on four different axial planes. Imaging at different axial depths requires modifying the divergence of each beamlet with added optics to cause a slight divergence in the beam as it reaches the objective back aperture. The system is capable of acquiring 250 frames per second on a single imaging plane (512 x 512 pixels) or 60 volumes per second for multi-plane imaging⁸. Implementing a multifocal system with more than four beamlets simply requires additional beam splitters and a laser of suitable pulse repetition rate and sufficient power to produce the beamlets^{14,15}.

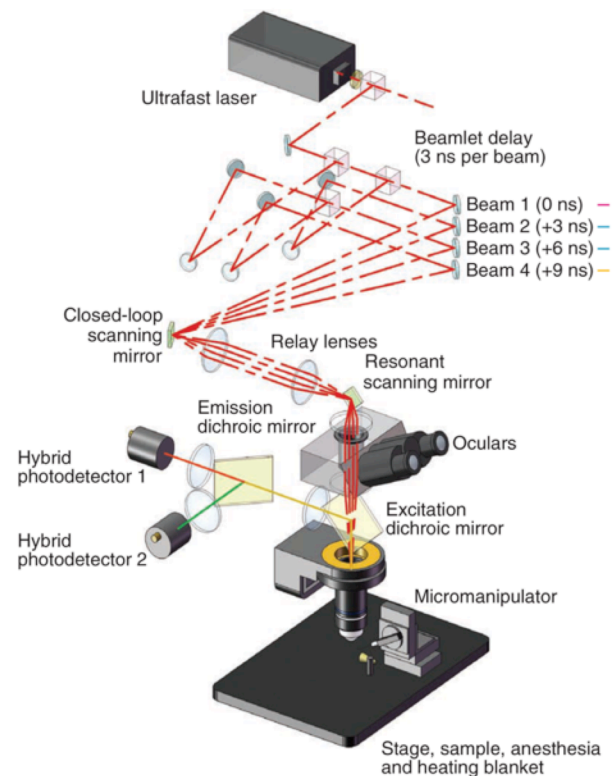


Figure 1 – Optical design of the spatiotemporal multiplexing two-photon calcium imaging system⁸.

Question 2

Calcium imaging is a noninvasive technique for indirectly monitoring neuronal activity by tracking changes in calcium concentration that occur as a result of action potentials in neurons⁶. Ca^{2+} concentration changes rapidly as action potentials are transmitted between chemical synapses through the function of voltage-gated Ca^{2+} channels¹⁶. Up until the past decade, the primary strategy for obtaining neural activity data has been electrophysiological studies involving the implantation of large-scale electrodes directly on the surface of the brain via highly invasive procedures¹⁷. Such techniques are only capable of resolving large-scale neural network activity rather than the highly localized connectivity of neurons¹⁸. Conventional single-photon optical methods have severely limited depth penetration because of the high scattering and absorption properties of brain matter and often relied upon the genetic insertion of fluorescent proteins into structures of interest^{19,20}. The advent of multi-photon microscopy ushered in a resurgence of optical calcium imaging development because of its ability to resolve single cells and to selectively target excitation light within small focal volumes^{21,22}. The predominate challenge with using two-photon microscopy for *in vivo* calcium imaging is the poor temporal resolution of most systems¹. This problem arises from the need to raster scan the two-photon illumination beam across the entire imaging area in order to generate the fluorescence image. Unfortunately, the calcium concentration changes can occur on the order of milliseconds, much faster than the time necessary to generate the typical full field-of-view two-photon image¹. In response to this problem, two different strategies have been developed: 1) increasing the speed of the scanning mechanism and 2) increasing the number of beams illuminating the sample.

While there have been numerous advances towards improving the speed of monofocal two-photon beam scanning, the techniques have often been accompanied by significant disadvantages. Targeted path scanning (TPS) has been utilized to greatly improve the efficiency of conventional galvanometers by optimizing the beam scanning to only target user-defined areas of interests (i.e. neurons rather than the background) to achieve speeds up to 100Hz²³. Unfortunately, TPS is still fundamentally limited by the inertia of the galvanometer and is unlikely to offer further improvements in scanning speed. A more recently developed technique utilizing acousto-optic deflectors (AODs) offers an inertia-free means of spatially controlling an optical beam without the use of any mechanical components^{24,25}. Pairs of AODs and pairs of orthogonal pairs of AODs are capable of steering a two-photon beam in 2D and 3D, respectively^{4,26}. AODs control the beams by manipulating the amplitude and frequency of a standing ultrasound wave, thus making random-access scanning feasible with microsecond response times and up to 500Hz imaging speeds²⁴. Unfortunately, the use of AODs severely limits the imaging depth ($\sim 200\mu\text{m}$) and field of view ($\sim 50\mu\text{m}$) of the two-photon system because of spatiotemporal dispersions introduced by the device². While corrections are possible with acousto-optic modulators (AOMs) and prism compensations, the current generation of AODs can not yet optimally image neural activity^{2,5}.

Cheng, et al. is the first group to implement a multifocal two-photon calcium imaging system and achieved imaging rates of up to 250Hz⁸. The development of multifocal two-photon systems has progressed through numerous beam splitting techniques including: microlens arrays²⁷, rotating lens⁷, cascaded beam-splitters^{9,28}, diffractive optics²⁹, and even custom multibeam laser oscillators³⁰. Regardless of the implementation, all multifocal systems have still relied upon inertia-limited galvanometers for scanning the multiple focal points across the object of interest, limiting their full potential. Several previous systems also depend upon spatially sensitive imaging devices such as CCDs because the individual beams are incident upon the sample simultaneously and are thus impossible to demultiplex^{9,31}. This severely degrades the performance of the imaging system because the resulting images are highly influenced by scattering. Temporally multiplexed systems, such as in this paper, utilize point detectors, which infer spatial information from the focal point targeting rather than the location of incident emission photons and are therefore minimally impacted by scattering⁸.

With the exception of the 4-AOD system, axial movement and true 3D imaging has been achieved either by moving the objective with piezoelectrodes^{3,9,32} or by manipulating the divergence of the excitation light^{8,33}. The motion involved with raising and lowering the objective could detrimentally affect the imaging process and is inertia-limited by the weight of the objective. The system developed by Cheng, et al. allows for the positioning of individual beamlets on different imaging planes but requires the addition of divergence optics in each beam's path, making it virtually impossible to change the exact axial position "on-demand" during an experiment⁸. Combining the multifocal system with AODs for axial targeting could possibly offer the first "true" 3D two-photon calcium imaging system by allowing for rapid transverse scanning via the multiple beamlets and highly selective depth imaging with the use of the acoustic deflector.

Question 3

The detector utilized in Cheng, et al. was a “state-of-the-art” hybrid photodetector (HPD) made by Hamamatsu Photonics that is essentially a combination of a photomultiplier tube (PMT) and an avalanche photodiode (APD)⁸. It contains a photocathode for converting incident photons into electrons, which are then accelerated by an electric field onto an avalanche diode (AD) as an electron bombardment target. PMTs have been the gold standard of low noise, high sensitivity point detectors for many years and one of the few surviving vacuum tube devices in today’s semiconductor world. They are capable of detecting very fast (rise and fall times of hundreds of picoseconds) and very weak optical signals with low dark current and incredibly high gain ($\sim 10^6$) achieved by accelerating photoelectrons in an electric field for impact on a series of dynodes^{34,35}. Because PMTs feature such high gains they are extremely sensitive to light and are easily saturated and/or damaged in the presence of too much light, severely limiting their applications^{35,36}. They also suffer from relatively poor quantum efficiency (~ 0.25) despite their high sensitivity. APDs are functionally the semiconductor analog of the PMT and are typically utilized when the light levels are too low for a standard photodiode but too bright for a PMT. They use the photoelectric effect to convert incident photons to electrons and then amplify the signal ($\sim 100x$) via avalanche multiplication within the semiconductor structure³⁵. While APDs have higher quantum efficiency (0.6-0.8) and are not susceptible to damage under bright light conditions, they suffer from higher dark currents compared to PMTs.

The HPD utilized in Cheng, et al. contains the photocathode and accelerating electric field found in a PMT and the AD found in an APD (**Fig. 2**). The GaAsP photocathode (0.45 quantum efficiency) converts incident photons into photoelectrons via the photoelectric effect, which are then accelerated and focused by an electric field onto an AD^{10,11}. The electrons impact the AD, producing thousands of electron-hole pairs (electron bombardment gain) for an incredibly high first stage gain ($\sim 1600x$). The free electrons then move through the high electric field of the AD and undergo avalanche multiplication by impact ionization ($\sim 110x$). The total gain of the HPD is $\sim 10^5$, approaching that of a PMT and easily supplemented with a preamplifier. The massive first stage gain of the HPD allows for very strong pulse height definition (better than PMT or APD) and very low excess noise factor^{8,35}. The rise/fall times of the HPD is on the order of hundreds of picoseconds with temporal resolution of 60-90ps, depending on the spatial location of the incident photon on the photocathode¹¹. The very short deadtime means that the HPD will not saturate as quickly as a PMT or APD, which is very important for imaging. Unfortunately, there are several drawbacks to the HPD including being relatively expensive, having high dark count rates that results in lower contrast, mediocre quantum efficiency, no sensitivity above 750nm with the GaAsP photocathode, and requiring two high voltage power supplies ($+400V$ and $-8kV$)^{10,11}.

The HPD offers the incredibly fast temporal resolution and minimal deadtime necessary to correctly detect the individual beamlet fluorescence emission events. It features a large gain that is easily amplified to compare with that a PMT and is therefore capable of single-photon detection. It is much less susceptible to saturation than a PMT, which is desirable given the potential for large ranges of emission photons during calcium imaging⁸. As a point detector, it does not suffer from the spatiotemporal ambiguity that a wide-field detector such as a CCD might experience during calcium imaging. CCDs are incapable of providing timing information regarding individual photons and would provide a time-integrated image of fluorescence depending on the speed of the device¹⁰. Wide-field detectors also suffer considerably from the effects of scattering, which severely impairs the spatial resolution of the resulting image and eliminates the benefits of selective illumination offered by two-photon microscopy⁸. If the HPD were not utilized, a modern-era PMT would probably be implemented in its place but with slightly reduced temporal resolution and safeguards to prevent saturation or damage.

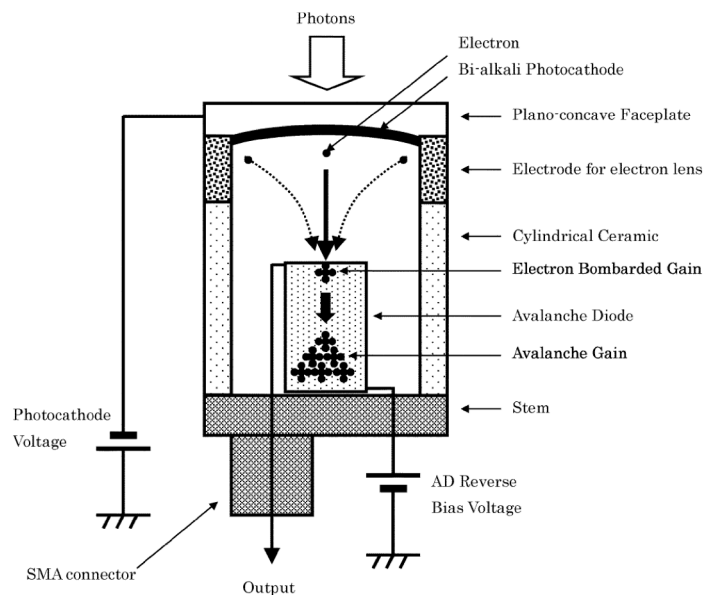


Figure 2 - Structure of the HPD¹¹.

Question 4

Cheng, et al. present the first multifocal two-photon calcium imaging system that is capable of imaging up to four axial planes simultaneously and offers a substantial increase in imaging speed compared to the standard two-photon microscope⁸. Unfortunately, the design remains fundamentally limited on several fronts, most importantly the use of “slow” galvanometric scanning mirrors. The physical movement of mirrors required to steer the reflected laser beamlets has an inertia-limited maximum speed that constrains the system from achieving faster scanning rates¹. While capable of imaging 2D planes at 250Hz and 3D volumes at 60Hz, the neural activity being observed occurs on the order of milliseconds and therefore could easily be missed. The authors acknowledge that the use of inertia-free AODs could drastically improve the scanning speeds but at the expense of optical strength and undesirable spatiotemporal dispersion of the beamlets^{24,25}. An easily implemented feature that could offer considerable improvements in scanning speeds even with the galvanometers is targeted path scanning (TPS)²³. Rather than raster scanning over the entire field-of-view, the scanning could be optimized to only illuminate neurons and thereby considerably increase the overall imaging speed. The reduction could be very drastic if only a few neurons are visible within the imaging window and the full 512x512 point scan were no longer necessary. Combined with the random-access capabilities of the AOD, TPS could easily offer an order of magnitude increase in frame illumination speeds for rapid two-photon calcium imaging.

Another major disadvantage of the technique presented by Cheng, et al. is the fixed axial depth of the individual beamlets that drastically reduces the axial sampling rate. The only options for changing the axial depth are manually adjusting the objective or moving the focusing optics that allow for the multi-plane focus. Neither is a viable option during a “live” experiment since adjusting the objective could disrupt the biological process being imaged and manipulating the optics requires high precision to maintain the beam spacing and desired axial offset. The beam must also be carefully controlled to ensure uniform delivery of optical power to each plane regardless of the depth. The total axial spacing is also fundamentally limited by the spherical aberration of the objective lens⁸. Because the focal point of each beamlet must be sufficiently separated in space to prevent overlap of focal volumes, the distance between each axial plane (~50µm) could result in missing activity that occurs between layers. Unfortunately, since the axial beam locations are essentially fixed, the system does not offer fully 3D scanning access into the specimen volume and is instead limited to only scanning up to four planes in two dimensions. The addition of multiple AODs could offer the ability to scan in all three dimensions but would require separate scanning setups for each beamlet, resulting in an explosive increase in cost and complexity⁴. The spatiotemporal dispersion and limited depth penetration problems associated with AODs would then have to be taken into account^{4,24-26}.

The photodetector used in the system also has several drawbacks as discussed previously. The HPD has virtually no sensitivity above 750nm because of its GaAsP photocathode material¹¹. Although this may not impair detection for current two-photon calcium indicators, it is possible that longer wavelength fluorescent probes might be undetectable. The spatiotemporal multiplexing also creates the potential for crosstalk between beamlets. Crosstalk occurs when the light cones from two neighboring beams overlap above and below the plane of focus resulting in erroneous two-photon excitation⁹. While Cheng, et al. claim that the crosstalk is negligible within their system, they do characterize the crosstalk leak-through to be $3.0 \pm 4.1\%$, which seems significant enough to possibly affect measurements⁸. They also opted to only utilize two beams when demonstrating the axial imaging of two separate planes simultaneously because of the increased likelihood for crosstalk. Another potential drawback is the susceptibility of the image processing to animal or instrument movement during data collection. Since the event localization algorithm depends heavily upon the spatial coordinates of the identified cells within each frame, any movement could skew the final connectivity diagram and therefore the interpretation of the event timing. Implementing a motion correction system would be a feasible improvement to their existing software and help make their technique more robust to normal biological movement caused by blood flow.

Another drawback of the system is the large area required to contain the temporal delay optics, which necessitates an almost 9m path to achieve the 9ns delay for the fourth beamlet⁸. Older systems have achieved spatiotemporally separated beamlets without the need for such expansive optical space, albeit without the same control over spatial and temporal positioning^{13,30}. This is a severe constraint on expanding the system to include more beamlets since additional beams would require even longer optical paths. Another problem with expanding the system is the need for lasers with lower repetition rates in order to allow for additional beam splitting^{14,15}. The 80MHz Ti:Al₂O₃ laser utilized in the paper can only properly handle four separate beams because of its 12.5ns pulse separation⁸. Further splitting of the main beam could also result in beamlets that are underpowered for properly exciting the fluorescent calcium indicators within the focal volume.

Question 5

The instrument designed by Cheng, et al. was utilized to demonstrate *in vivo* calcium imaging at two different axial positions within an intact mouse brain in order to monitor the local network activity of neurons⁸. Using the two-photon calcium indicator Fluo-4 AM in anesthetized mice, they imaged Layer 2/3 (L2/3) of the somatosensory barrel cortex to determine whether spontaneous activity spread in a “columnar” fashion as previously reported¹². Columnar refers to coordinated neural activity arranged vertically across the layers of the brain rather than laterally across the same layer of the cortex or randomly across both. In 2003, Cossart, et al. found that unstimulated neural activity in slices of mouse visual cortex occurred in “spatially organized ensembles” involving only a few neurons¹². They determined that synchronized neuronal events (peaks of synchrony) were typically spatially structured and only involved about 2.2% of all imaged cells. The four spatial structures identified and their frequency of occurrence were: random distributions (74%), clusters (19%), layers (4%), and columns (3%)¹². The very low occurrence rate for columnar activity seems to contradict the stated motivation behind the experiment being performed by Cheng, et al, who are examining whether columnar neural activity can occur in the brain.

The two-photon calcium imaging was carried out in L2/3 of the barrel cortex using two imaging planes axially separated by 50 μ m, each with two simultaneous excitation beamlets⁸. The fluorophore Fluo-4 AM was injected into postnatal anesthetized (0.5-1% isoflurane) mice and used to track spontaneous neural activity via calcium transients. Cells participating in peaks of synchrony were identified and used to generate connectivity diagrams based on peak correlation coefficients between pairs of cells from each of the two depths. It was determined that only a small minority of all activity bursts had the wide axial and narrow radial spread (**Fig. 3**) that would be consistent with columnar connectivity, which actually agrees with the results of Cossart, et al. despite the assertion that it does not^{8,12}. Similarly, only a few instances corresponded to the layered and clustered organization schema previously mentioned. The majority of the activity bursts were defined by distributions that were wide in both the axial and radial dimensions, indicating predominately randomly dispersed activity. These results agree convincingly with those previously obtained using visual cortex slices and confirms that the majority of coordinated spontaneous neural activity occurs in a mostly randomly distributed spatial structure rather than in a columnar fashion. This extremely random distribution of spontaneous activity illustrates the incredibly interconnected neural network contained within the brain. It also provides an excellent baseline for future studies that examine the stimulated neural activity response within the same region.

While the general results of Cheng, et al. agree with those found by Cossart, et al., there are still several potential problems with the *in vivo* experiment. The most important is the decision to image only two planes of neural activity rather than all four that the multiplexed two-photon system is capable of achieving. This severely limited the axial activity sampling compared to the sagittal cortical slices used in the previous experiment. Extensive axial sampling should have been the priority given the motivation of examining columnar neural activity. While ultimately the end results do agree, it is entirely possible that the limited axial information has drastically influenced the actual dynamics of spontaneous neural activity. Additional experiments should be conducted using all four focal planes to better ascertain the true nature of columnar coordination. Another potential problem is the use of anesthesia during the neural activity experiments. Anesthesia has been shown to affect functional imaging results, predominately by decreasing the magnitude of neural responses compared to that of an awake animal³⁷. While it is impractical to use two-photon calcium imaging on a conscious animal, future studies must be carefully constructed to optimize the anesthesia levels such that the animal provides the least dampened response possible.

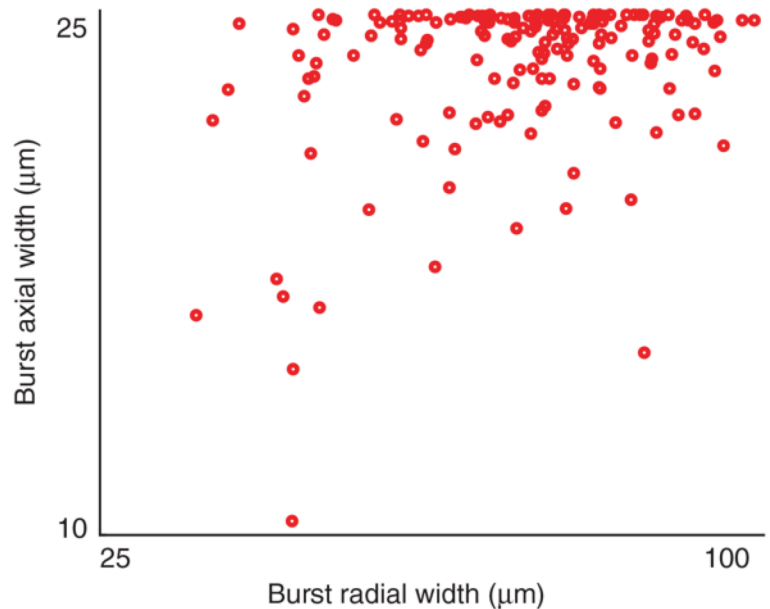


Figure 3 - Neural activity burst spatial distribution⁸.

References

1. Svoboda, K. & Yasuda, R. Principles of two-photon excitation microscopy and its applications to neuroscience. *Neuron* **50**, 823–839 (2006).
2. Kremer, Y. *et al.* A spatio-temporally compensated acousto-optic scanner for two-photon microscopy providing large field of view. *Opt. Express* **16**, 10066–10076 (2008).
3. Göbel, W., Kampa, B. M. & Helmchen, F. Imaging cellular network dynamics in three dimensions using fast 3D laser scanning. *Nat. Meth.* **4**, 73–79 (2006).
4. Duemani Reddy, G., Kelleher, K., Fink, R. & Saggau, P. Three-dimensional random access multiphoton microscopy for functional imaging of neuronal activity. *Nat. Neurosci.* **11**, 713–720 (2008).
5. Grewe, B. F., Langer, D., Kasper, H., Kampa, B. M. & Helmchen, F. High-speed in vivo calcium imaging reveals neuronal network activity with near-millisecond precision. *Nat. Meth.* **7**, 399–405 (2010).
6. Grewe, B. F. & Helmchen, F. Optical probing of neuronal ensemble activity. *Curr. Opin. Neurobiol* **19**, 520–529 (2009).
7. Bewersdorf, J., Pick, R. & Hell, S. W. Multifocal multiphoton microscopy. *Opt. Lett.* **23**, 655–657 (1998).
8. Cheng, A., Gonçalves, J. T., Golshani, P., Arisaka, K. & Portera-Cailliau, C. Simultaneous two-photon calcium imaging at different depths with spatiotemporal multiplexing. *Nat. Meth.* **8**, 139–142 (2011).
9. Nielsen, T., Fricke, M., Hellweg, D. & Andresen, P. High efficiency beam splitter for multifocal multiphoton microscopy. *J. Microsc.* **201**, 368–376 (2001).
10. Michalet, X. *et al.* Hybrid photodetector for single-molecule spectroscopy and microscopy. 68620F (2008).doi:10.1117/12.763449
11. Fukasawa, A., Haba, J., Kageyama, A., Nakazawa, H. & Suyama, M. High Speed HPD for Photon Counting. *IEEE Trans. Nucl. Sci.* **55**, 758–762 (2008).
12. Cossart, R., Aronov, D. & Yuste, R. Attractor dynamics of network UP states in the neocortex. *Nature* **423**, 283–288 (2003).
13. Ji, N., Magee, J. C. & Betzig, E. High-speed, low-photodamage nonlinear imaging using passive pulse splitters. *Nat. Meth.* **5**, 197–202 (2008).
14. Theer, P., Hasan, M. T. & Denk, W. Two-photon imaging to a depth of 1000 μm in living brains by use of a $\text{Ti:Al}_2\text{O}_3$ regenerative amplifier. *Opt. Lett.* **28**, 1022 (2003).
15. Ramaswamy, M., Ulman, M., Paye, J. & Fujimoto, J. G. Cavity-dumped femtosecond Kerr-lens mode-locked $\text{Ti:A1}_2\text{O}_3$ laser. *Opt. Lett.* **18**, 1822–1824 (1993).
16. Silbernagl, S. & Despopoulos, A. Chapter 2: Nerve and Muscle, Physical Work. *Color Atlas of Physiology* 42–56 (2009).
17. Churchland, M. M., Yu, B. M., Sahani, M. & Krishna V Shenoy Techniques for extracting single-trial activity patterns from large-scale neural recordings. *Curr. Opin. Neurobiol* **17**, 609–618 (2007).
18. Kerr, J. N. D. & Denk, W. Imaging in vivo: watching the brain in action. *Nat. Rev. Neurosci.* **9**, 195–205 (2008).
19. Helmchen, F., Imoto, K. & Sakmann, B. Ca^{2+} buffering and action potential-evoked Ca^{2+} signaling in dendrites of pyramidal neurons. *Biophys. J.* **70**, 1069 (1996).
20. Wilt, B. A. *et al.* Advances in Light Microscopy for Neuroscience. *Annu. Rev. Neurosci.* **32**, 435–506 (2009).
21. Zipfel, W. R., Williams, R. M. & Webb, W. W. Nonlinear magic: multiphoton microscopy in the biosciences. *Nat. Biotechnol.* **21**, 1369–1377 (2003).
22. Kerlin, A. M., Andermann, M. L., Berezovskii, V. K. & Reid, R. C. Broadly tuned response properties of diverse inhibitory neuron subtypes in mouse visual cortex. *Neuron* **67**, 858–871 (2010).
23. Lillisa, K. P., Enga, A., Whitea, J. A. & Mertz, J. Two-photon imaging of spatially extended neuronal network dynamics with high temporal resolution. *J. Neurosci. Methods* **172**, 178–184 (2008).
24. Salomé, R. *et al.* Ultrafast random-access scanning in two-photon microscopy using acousto-optic deflectors. *J. Neurosci. Methods* **154**, 161–174 (2006).
25. Iyer, V., Hoogland, T. M. & Saggau, P. Fast Functional Imaging of Single Neurons Using Random-Access Multiphoton (RAMP) Microscopy. *J. Neurophysiol.* **95**, 535–545 (2006).
26. Lv, X., Zhan, C., Zeng, S., Chen, W. R. & Luo, Q. Construction of multiphoton laser scanning microscope based on dual-axis acousto-optic deflector. *Rev. Sci. Instrum.* **77**, 046101 (2006).
27. Buist, A. H., Müller, M., Squier, J. A. & Brakenhoff, G. J. Real time two-photon absorption microscopy using multi point excitation. *J. Microsc.* **192**, 217–226 (1988).
28. Fittinghoff, D., Wiseman, P. & Squier, J. A. Widefield multiphoton and temporally decorrelated multifocal multiphoton microscopy. *Opt. Express* **7**, 273–279 (2000).
29. Sacconi, L. *et al.* Multiphoton multifocal microscopy exploiting a diffractive optical element. *Opt. Lett.* **28**, 1918–1920 (2003).
30. Sheetz, K. E., Hoover, E. E., Carriles, R., Kleinfeld, D. & Squier, J. A. Advancing multifocal nonlinear microscopy: development and application of a novel multibeam $\text{Yb:KGd(WO}_4)_2$ oscillator. *Opt. Express* **16**, 17574–17584 (2008).
31. Kim, K. H. *et al.* Multifocal multiphoton microscopy based on multianode photomultiplier tubes. *Opt. Express* **15**, 11658 (2007).
32. Chandler, E. *et al.* High-resolution mosaic imaging with multifocal, multiphoton photon-counting microscopy. *Appl. Opt.* **48**, 2067–2077 (2009).
33. Duocastella, M., Sun, B. & Arnold, C. B. Simultaneous imaging of multiple focal planes for three-dimensional microscopy using ultra-high-speed adaptive optics. *J. Biomed. Opt.* **17**, 050505–050505–3 (2012).
34. Arisaka, K. Principle of PMT and Its Calibration. *PMT Calibration School* 63 (2003).at <http://www.physics.ucla.edu/~arisaka/auger/energy/pmt_basics.pdf>
35. Hobbs, P. C. D. Chapter 3: Optical Detection. *Building Electro-Optical Systems* 91–144 (2009).
36. Davis, M. A. Concerning the performance of photodetectors. (2012).
37. Martin, C., Martindale, J., Berwick, J. & Mayhew, J. Investigating neural–hemodynamic coupling and the hemodynamic response function in the awake rat. *NeuroImage* **32**, 33–48 (2006).